Dalton
www.rsc.org/dalton

Synthesis, characterization and reactivity of *trans*-[RuCl(NO)(bpydip)]$^{2+}$ {bpydip = *N*,*N*′-bis(7-methyl-2-pyridylmethylene)-1,3-diiminopropane}: a novel nitrosyl ruthenium complex displaying high electronic delocalization

Vagner Roberto de Souza, Ana Maria da Costa Ferreira and Henrique Eisi Toma *
Departamento de Química Fundamental, Instituto de Química, Universidade de São Paulo, Caixa Postal 26077, CEP 05513-970, São Paulo, SP, Brazil. E-mail: henetoma@iq.usp.br

Received 8th May 2002, Accepted 25th November 2002
First published as an Advance Article on the web 2nd January 2003

A novel *trans*-[RuCl(NO)(bpydip)]$^{2+}$ species has been obtained by the reaction of nitrite ions with *trans*-[RuCl$_2$(bpydip)] {bpydip = *N*,*N*′-bis(7-methyl-2-pyridylmethylene)-1,3-diiminopropane}, and extensively characterized by means of elemental analysis, cyclic voltammetry, UV/Visible, FTIR, ^{1}H NMR and EPR spectroscopy. The electrochemistry in acetonitrile solution, consists of two sets of reversible redox processes ascribed to the Ru$^{III/II}$ ($E_{1/2}$ = +1.92 V *versus* NHE) and NO$^{+/\bullet}$ ($E_{1/2}$ = +0.34 V) redox couples. A relatively high ν(NO) stretching frequency (1920 cm^{-1}) has been observed in the FTIR spectra, indicating a NO$^+$ character, while the absence of EPR signals is also consistent with the Ru^{II}–NO$^+$ formulation. The reduction of the complex was monitored spectroelectrochemically, exhibiting a shift of ν(NO) to 1890 cm^{-1}; and giving rise to characteristic EPR signals which evidence the NO$^\bullet$ character in the product. The nitrosyl (NO$^+$) species reacts with H$_2$O according to the equation [RuCl(NO)(bpydip)]$^{2+}$ + H$_2$O ⟶ [RuCl(NO$_2$)(bpydip)] + 2H$^+$, leading to a pseudo-first order rate constant of 1.40 (± 0.02) × 10^{-2} s^{-1}, $\Delta H^{\neq}$ = 47 (± 1) kJ mol^{-1} and $\Delta S^{\neq}$ = 122 (± 4) J K^{-1} mol^{-1}.

Introduction

Interest in the chemistry of NO, and ruthenium nitrosyl complexes in particular,[1–6] has intensified in recent years because of its role and implications in numerous physiological functions.[7–11] The multifacet biological importance of NO can be separated into three categories including protective, regulatory and deleterious.[12] Protective effects include nitric oxide as an antioxidant agent and inhibitor to leukocyte adhesion. Among the many regulatory effects of NO are its ability to control vascular tone and permeability, cellular adhesion and renal function. Nitric oxide has been established as a neurotransmitter, bronchodilator and inhibitor of platelet aggregation. In addition, NO is the final common effector molecule of nitrovasodilators, activating guanylyl cyclase. Nitric oxide also has several deleterious effects, inhibiting some enzymes and inducing DNA damage and lipid peroxidation.[13,14] The development of metal nitrosyl complexes having a high degree of electrophilic character of the coordinated NO function[15] is another relevant point, since the electrophilic NO$^+$ centre is susceptible to molecular transformations in contact with nucleophiles.[5,6,15] In fact, in this regard, nitrosyl complexes have been increasingly studied, exploiting the dependence of the NO behavior on the nature of the ancillary groups attached to the metal center.[16–21]

These aspects have prompted us to investigate the ruthenium nitrosyl complex with the tetradentate Schiff base ligand, *N*,*N*′-bis(7-methyl-2-pyridylmethylene)-1,3-diiminopropane (bpydip), illustrated in Fig. 1. Although ruthenium derivatives containing Schiff base ligands are not unusual,[5,6,22] to our knowledge there are no reports in the literature on the corresponding N$_4$ tetradentate Schiff base complexes. This ligand has two α,α'-diimine fragments, a characteristic which can be further exploited, by analogy with α,α'-diimine complexes of ruthenium(II), in photo-induced charge-transfer processes.[23]

DOI: 10.1039/b204419f

Experimental

Materials

The tetradentate Schiff base ligand was obtained *in situ* by condensation of 2-acetylpyridine (Aldrich) with 1,3-diaminopropane (Aldrich) in ethanol.[24] RuCl$_3$·3H$_2$O (Aldrich) was the starting material for the synthesis of the ruthenium complex. All other solvents and chemicals were reagent grade and were used as supplied.

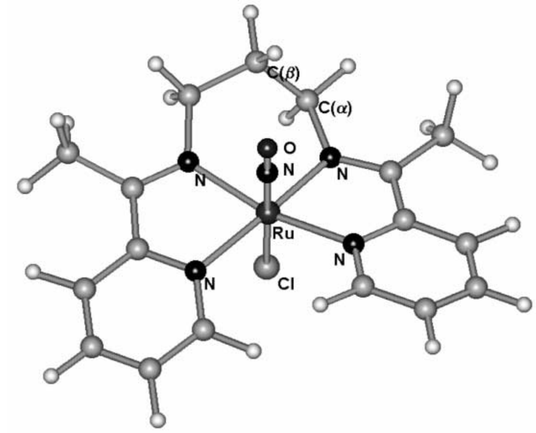

Fig. 1 MM$^+$ structural representation of *trans*-[RuCl(NO)(bpydip)]$^{2+}$, showing the labels employed in the 2D COSY ^{1}H NMR assignment.

Synthesis of ruthenium complexes

***trans*-[RuCl$_2$(bpydip)].** RuCl$_3$·3H$_2$O (0.25 g, 1 mmol) and LiCl (1 g) were dissolved in ethanol (25 cm^3) and the mixture was heated to reflux for 30 min. In separate, a mixture of 2-acetylpyridine (0.12 g, 1 mmol) and 1,3-diaminopropane (0.038 g, 0.5 mmol) in ethanol (10 cm^3) was heated to reflux for 45 min, and then carefully transferred to the ruthenium chloride flask. Immediately, a deep blue solution resulted, which was further refluxed for 2 h. After evaporation of the solvent under reduced pressure, the *trans*-[RuCl$_2$(bpydip] complex was purified by chromatography, using an Al$_2$O$_3$ column, and acetonitrile as eluent.[25] The green fraction was evaporated to dryness, and kept under vacuum. Yield 0.10 g (23%). (Found: C, 45.10; H, 4.49; N, 12.31. Calc. for RuC$_{17}$H$_{20}$N$_4$Cl$_2$: C, 45.13; H, 4.46; N, 12.39%.) ν_{max}/cm^{-1}: 1590s (C=N); 262w (Ru–Cl).

***trans*-[RuCl(NO)(bpydip)](PF$_6$)$_2$.** *trans*-[RuCl$_2$(bpydip)] (0.10 g, 0.2 mmol) was dissolved in deaerated water (5 cm^3), and 0.1 cm^3 of 2 mol dm^{-3} HCl was added. An aqueous NaNO$_2$ solution (0.03 g, 0.4 mmol) was added dropwise to the stirred solution over a 10 min period. After complete addition, the brown solution was warmed at 50 °C for an additional 10 min. An excess of saturated aqueous NaPF$_6$ solution was slowly added to the solution giving a pale brown precipitate. The solid was collected on a filter, washed with cold water, and dried in air. Yield 0.15 g (90%). (Found: C, 27.63; H, 2.78; N, 9.45. Calc. for RuC$_{17}$H$_{20}$N$_5$OClP$_2$F$_{12}$: C, 27.70; H, 2.74; N, 9.50%.) ν_{max}/cm^{-1}: 1920s (NO); 1597s (C=N).

Physical measurements

Elemental analyses were performed at the local Analytical Center, using a Perkin-Elmer 2400 CHN Elemental Analyser. Electronic spectra were recorded on a Hewlett-Packard model 8452-A diode array spectrophotometer. IR spectra were recorded on a Shimadzu FTIR-8300 spectrophotometer. ^{1}H NMR spectra were obtained using a Varian Inova 300 MHz spectrometer, in CDCl$_3$ or acetone-d$_6$. EPR spectra were recorded on a Bruker EMX X-band spectrometer at 77 K. EPR spectra were also recorded after the reduction of *trans*-[RuCl(NO)(bpydip)](PF$_6$)$_2$ by Zn amalgam, in acetonitrile solution. The sample was frozen in liquid N$_2$ immediately after the preparation, and the EPR spectra recorded at 9.43 GHz, 1 mW power, and 3.9 G modulation amplitude. Cyclic voltammetry measurements were carried out using a PARC system, from EG&G instrument, consisting of a potentiostat model 283, and a three electrode cell arrangement. The software ECHEM, version 4.30, was used. Solutions of ruthenium complexes (5 mmol dm^{-3}) were prepared in acetonitrile, containing 0.1 mol dm^{-3} tetraethylammonium perchlorate. A platinum disc working electrode and a platinum wire auxiliary electrode were employed for the measurements *vs.* an Ag/AgNO$_3$ reference electrode {E^0 = 0.503 V *vs.* NHE}.[26] UV/Visible spectroelectrochemical measurements were carried out using a PARC potentiostat, model 173, in parallel with a Hewlett-Packard diode array spectrophotometer (model 8453). The quartz spectroelectrochemical cell used has a 0.025 cm optic length. A gold minigrid working electrode and a platinum auxiliary microelectrode were employed in these measurements *vs.* an Ag/AgNO$_3$ reference minielectrode. FTIR spectroelectrochemistry was carried out using the PARC potentiostat and the Shimadzu spectrophotometer. The spectroelectrochemical cell was assembled using two IRTRAN© windows, as previously described.[27]

The *trans*-[RuCl(NO)(bpydip)]$^{2+}$ ⟶ *trans*-[RuCl(NO$_2$)-(bpydip)] reaction was monitored spectrophotometrically (λ_{max} = 530 nm) at several temperatures, in acetonitrile, by adding fifty times excess of water, in relation to the complex. The kinetic study of the reaction of *trans*-[RuCl(NO)(bpydip)]$^{2+}$ with acetone in the presence of amines was monitored spectrophotometrically (λ_{max} = 550 nm). In both cases, for the determination of k, the absorbance increase (A_t) at 550 nm (or at 530 nm, corresponding to λ_{max} of the nitro species) was recorded as a function of time (t). Values of pseudo-first order rate constants, k, were obtained from the slopes of linear least-squares plots of $\ln(A_\infty - A_0)/(A_\infty - A_t)$ against t. The activation parameters $\Delta H^{\neq}$ and $\Delta H^{\neq}$ were determined from the corresponding Eyring plots.[28]

Molecular calculations

Semiempirical molecular orbital calculations were carried out by using the ZINDO/S method within the HyperChem 6.1 program from Hypercube. The default parameterization was based on the original ZINDO program package,[29] using as interaction factors, the universal values k_σ = 1.267 and k_π = 0.585. SCF molecular orbitals were obtained at the RHF level. Geometry optimizations were carried out using the ZINDO/1 methods with its resident parameters. The electronic spectra simulation was carried out using single excited configuration interaction, within an active space involving 8 occupied and 8 unoccupied molecular orbitals. Initial nuclear coordinates of the complex were given by molecular mechanics calculations employing the MM$^+$ module from Hyperchem, with a gradient of 1 × 10^{-5} kcal Å^{-1} as a convergence criterion in a conjugate gradient algorithm. All the calculations were performed on a PC Windows platform with a Pentium III microprocessor.

Results and discussion

^{1}H NMR spectra

^{1}H NMR and 2D COSY spectra were employed for the structural characterization of the *trans*-[RuCl(NO)(bpydip)]$^{2+}$ complex in solution. Unfortunately, all the attempts to obtain suitable crystals for X-ray studies have not been successful up to the present time.

The NMR spectrum of the compound is characterized by a relatively simple pattern of resonance signals, consisting of two doublets {H(6) = 9.60 ppm (2H); H(3) = 7.85 ppm (2H)} and two triplets {H(4) = 7.75 ppm (2H); H(5) = 7.30 ppm (2H)}, associated with the aromatic rings protons. The spectrum reveals that both pyridine moieties are equivalent, supporting an almost planar coordination geometry for the tetradentate ligand (C_1 symmetry on the ligand). According to the molecular simulations, the two pyridine rings swing away from each other in order to evade the intramolecular repulsion between two hydrogen atoms at the 6-position. This type of effect has also been previously reported for related complexes.[30] The methyl, α- and β-methylene resonances were observed at higher magnetic field and were assigned, from their relative areas, as CH$_3$ = 2.70 ppm (6H); H(α) = 4.62 ppm (4H) and; H(β) = 2.69 ppm (2H).

Electronic spectra

The electronic spectrum of the nitrosyl complex (Fig. 2) consists of a broad, weak absorption shoulder around 550 nm, overlapping a structured band centered at 470 nm (λ_{max} = 490, 460, 420 nm), in addition to a strong band at 397 nm and a shoulder at 358 nm. The spectrum is quite different from that of the *trans*-[RuCl$_2$(bpydip)] complex, which is characterized by a major, strong charge-transfer band at 644 nm associated with the Ru^{II}L chromophore. The assignment is complicated by the fact that NO is a typical non-innocent ligand, and its complexes

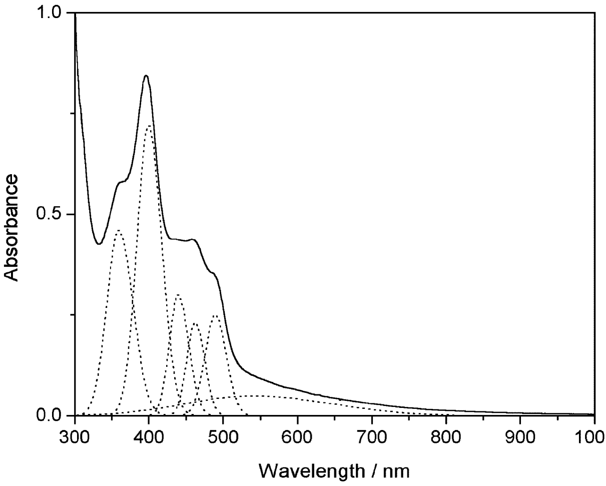

Fig. 2 Electronic spectra of the *trans*-[RuCl(NO)(bpydip)](PF$_6$)$_2$ in acetonitrile. [Ru]: 5 × 10^{-4} mol dm^{-3}.

Table 1 Energies and composition of the valence levels (ZINDO/S) for *trans*-[RuCl(NO)(bpydip)]$^{2+}$

MO	Energy/eV	Ru (%)	NO (%)	Cl (%)	Bpydip (%)
70	−0.271	18.9	8.4	0.2	72.4
69	−0.281	6.8	83.1	0.2	9.9
68	−0.298	2.5	1.3	0.4	95.8
67(LUMO)	−0.323	18.0	37.5	0.7	43.3
66(HOMO)	−0.523	31.4	27.4	1.2	40.5
65	−0.555	14.4	6.3	3.3	75.9
64	−0.569	52.3	10.1	0.2	37.3
63	−0.578	14.4	6.3	3.3	75.9
62	−0.582	15.9	6.0	2.5	75.6
61	−0.614	2.8	2.2	12.9	82.1

Table 2 Experimental and ZINDO/S calculated electronic transitions in the visible region, for *trans*-[RuCl(NO)(bpydip)]$^{2+}$

Experimental		Calculated	
λ_{max}/nm	ε/dm^3 mol^{-1} cm^{-1}	λ_{max}/nm	Transition
550	360	545	MO(66)⟶MO(69)
490	1330	472	MO(66)⟶MO(68)
460	1680		vibronic
420	1900	404	MO(64)⟶MO(69)
397	3240	385	MO(63)⟶MO(67)
358	2210	344	MO(62)⟶MO(67)

can exhibit NO$^+$, NO^0 or NO$^-$ character, depending on how its HOMO level matches the valence levels of the open shell transition metal ions.[31] For this reason, the assignment of the electronic spectrum of the *trans*-[RuCl(NO)(bpydip)]$^{2+}$ complex can not be carried out based on comparison with the *trans*-[RuCl(X)(bpydip)]$^{n+}$ series. Instead, theoretical calculations are required for this purpose.

In Table 1 one can find the results from the ZINDO/S calculations for *trans*-[RuCl(NO)(bpydip)]$^{2+}$. As one can see, the LUMO level (MO 67) is delocalized over the entire (bpydip)Ru(NO) system, although exhibiting a pronounced NO character (37.5%). MO 69, on the other hand is essentially NO (83.1%), while MO 68 and 70 are mainly localized on the bpydip ligand. Regarding the HOMO level (MO 66), the calculations show that it is highly delocalized over the (bpydip)Ru(NO) system. In contrast, the bpydip character predominates in MO 65 (75.9%), and the ruthenium character is particularly strong in MO 64 (52.3%).

The ZINDO/S calculated spectrum, fits reasonably well the experimental electronic transitions, as shown in Table 2. The absorption shoulder around 550 nm coincides with the theoretical weak transition at 545 nm, corresponding to MO 66⟶MO 69, or approximately, a metal-to-NO charge-transfer transition (MLCT). The absorption bands observed at 490 and 460 nm coincide with the theoretically expected MO 66⟶MO 68 transition at 472 nm, which corresponds to the transition from the delocalized LUMO level to an excited level essentially localized on the bpydip ligand (95.8%). This band corresponds to a metal-to-bpydip CT transition (MLCT). It should be noted that the peaks at 490 and 460 nm exhibit energy separation ($\Delta\nu$ = 1330 cm^{-1}) typical of vibrational levels in metal-diimine chromophores, thus suggesting a vibronic nature.

On the other hand, the electronic transition at 404 nm (MO 64⟶MO 69), can be described as a Ru⟶NO* MLCT transition. The remaining bands in the near-UV region, *i.e.*, at 397 (MO 63⟶MO 67) and 358 nm (MO 62⟶MO 67) correspond to MO transitions exhibiting significant bpydip⟶NO* character.

The results shown in Table 1 and 2, reveal a large participation of the NO ligand in the valence levels, thus explaining the unusual electronic absorption profile of the *trans*-[RuCl(NO)(bpydip)]$^{2+}$ complex.

IR spectra

The vibrational spectrum of the *trans*-[RuCl(NO)(bpydip)](PF$_6$)$_2$ complex is shown in Fig. 3.

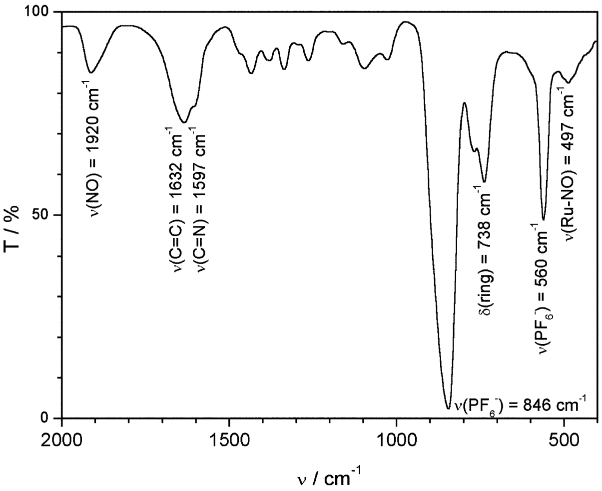

Fig. 3 Vibrational spectrum of the *trans*-[RuCl(NO)(bpydip)](PF$_6$)$_2$ in a KBr disc.

The most relevant peak is observed at 1920 cm^{-1}, corresponding to νNO. The strong peaks at 846 and 560 cm^{-1} are associated with the PF$_6^-$ asymmetric and symmetric stretching vibrations, while the remaining peaks can be ascribed to bpydip vibrational frequencies: 1632, 1597 (ν_{as}C=C, ν_{as}C=N), 1435 (ν_sC=C, ν_sC=N), 1337 (ν_sC=C), 1263 (δC=C), 1099 (δCH), 1026 (ring breathing), 775, 738 (δring). The weak vibrational peak at 497 cm^{-1} can be tentatively ascribed to νRu–NO.

It should be noticed that the ν(NO) peak of free NO is located at 1876 cm^{-1}, but in the metal complexes it is very sensitive to the binding properties and oxidation states of the metal ion. For instance, the typical ν(NO) frequencies for *cis*-[Ru^{II}(bipy)$_2$(NO)L] complexes (L = N$_3^-$, Cl$^-$, NO$_2^-$, NH$_3$, py, CH$_3$CN) complexes[32] have been observed in the range 1923–1970 cm^{-1}. For [Ru^{II}(NH$_3$)$_5$NO]$^{3+}$ and *trans*-[Ru^{II}(NH$_3$)$_4$(NO)L] complexes (L = imidazole, L-histidine, py, isonicotinamide, pyrazine, P(OEt)$_3$), ν(NO) span the range 1909–1941 cm^{-1}; but for L = SO$_3^{2-}$, ν(NO) = 1871 cm^{-1}.[17] In the case of *trans*-[Ru^{II}(py)$_4$(NO)L] complexes, for L = Cl$^-$ and Br$^-$, ν(NO) = 1910 and 1901 cm^{-1}, respectively, but for L = OH$^-$, ν(NO) = 1860 cm^{-1}.[22] In all such examples, the ruthenium center has been considered as mainly Ru^{II}, thus imputing a predominantly NO$^+$ character to the nitrosyl ligand. In the case of the reduced complexes, [Ru(bipy)$_2$(NO)(CH$_3$CN)]$^{2+}$ and [Ru(bipy)$_2$(NO)Cl]$^+$, ν(NO) is shifted to 1665 and 1640 cm^{-1}, and the spectroscopic and electrochemical data support the hypothesis of NO$^+$ reduction, yielding NO$^•$ species.[32]

Electrochemistry

A typical cyclic voltammogram of the *trans*-[RuCl(NO)(bpydip)](PF$_6$)$_2$ complex is shown in Fig. 4. By starting at 0.5 V and

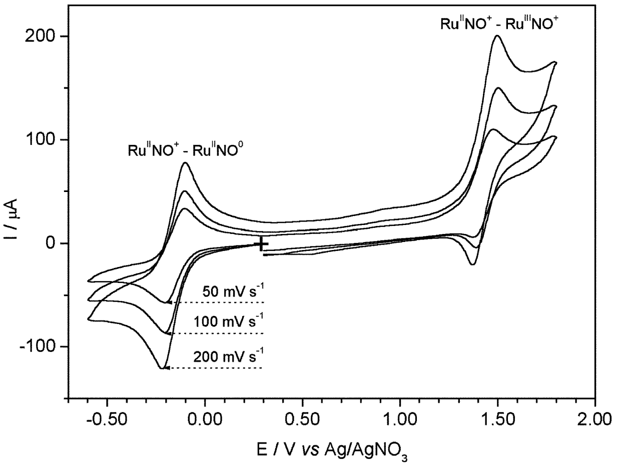

Fig. 4 Cyclic voltammograms of the *trans*-[RuCl(NO)(bpydip)](PF$_6$)$_2$ in acetonitrile. [Ru]: 1 × 10^{-3} mol dm^{-3}; working electrode: Pt; reference electrode: Ag/AgNO$_3$ (0.01 mol dm^{-3}); μ: 0.10 mol dm^{-3} with Et$_4$NClO$_4$; room temperature.

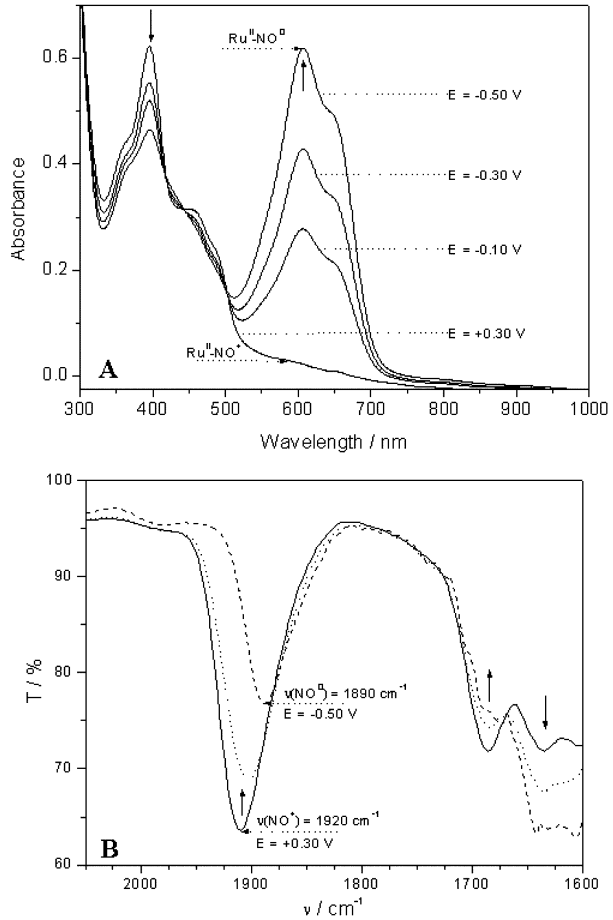

Fig. 5 UV-Vis (A) and FTIR (B) spectroelectrochemistry of *trans*-[RuCl(NO)(bpydip)](PF$_6$)$_2$ in acetonitrile. [Ru]: 1.0 10^{-3} mol dm^{-3}; working electrode: Pt; reference electrode: Ag/AgNO$_3$ (0.01 mol dm^{-3}); μ: 0.10 mol dm^{-3} with Et$_4$NClO$_4$; room temperature.

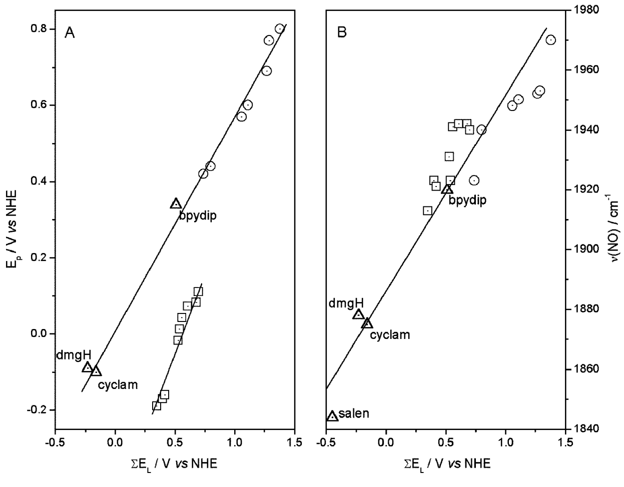

Fig. 6 (A) Correlation between $E_{1/2}$ and ΣE_L; (B) correlation between ν(NO) and ΣE_L for: △, *trans*-[RuCl(NO)(L)]$^{n+}$ (L = bpydip, cyclam,[3] dmgH,[27] salen[22]); ○, *cis*-[Ru(bpy)$_2$(NO)(L)]$^{n+}$ (L = N$_3^-$, Cl$^-$, NO$_2^-$, NH$_3$, terpy, py, CH$_3$CN)[35] and □, *trans*-[Ru(NH$_3$)$_4$(NO)(L)]$^{n+}$ (L = NH$_3$, imN, L-hist, py, isn, nic, pz, P(OEt)$_3$, P(OMe)$_3$).[36]

scanning in the direction of positive potentials, a reversible one-electron wave can be observed at $E_{1/2}$ = 1.92 V *vs.* NHE, associated with the Ru^{II}/Ru^{III} redox couple. It is important to note that the potential is shifted by 1.6 V, when the axial ligand is changed from chloride to NO$^+$ ion (*trans*-[RuCl$_2$(bpydip)]: $E_{1/2}$ = 0.30 V), reflecting the dramatic influence of the NO ligand in the complex.

By scanning in the direction of negative potentials, a second reversible one-electron wave can be observed at $E_{1/2}$ = 0.34 V *versus* NHE corresponding to the Ru^{II}–NO$^{+/\bullet}$ redox couple. Reversible monoelectronic reductions of the nitrosyl ligand have been reported in the range of −0.12 to 0.80 V, for ruthenium complexes containing a linear MNO group.[27,32,33] In our case, however, it is interesting to note that the reduction of the NO ligand occurs in the middle range of potentials, with good chances of being reduced by the biological reducing agents.[34] This process is accompanied by a dramatic change in UV/Visible spectra, as shown in Fig. 5A, exhibiting a decrease of the absorption bands below 500 nm, and the rise of a strong band at 608 nm (ε = 3500 dm^3 mol^{-1} cm^{-1}), characteristic of to metal-to-imine charge transfer transitions.[25]

By collecting the representative data for $E_{1/2}$(Ru^{II}–NO$^{+/\bullet}$) from the literature,[35,36] two sets of linear correlations with respect to Lever's parameters for the ligands, ΣE_L, can be observed, as shown in Fig. 6. It should be noticed that Lever's parameter for NO is not yet well established, because of the non-innocent character of the ligand. [37] Values varying from 1.3 to 2.5 has been suggested.[38] For correlation purposes, in analogy with the literature, [35,36] this value was not included in ΣE_L. The *trans*-RuCl(NO)(bpydip)]$^{2+}$ complex seems to fit the top line correlation, (Fig. 6A) in the same group of ruthenium(II)–polypyridine and ruthenium(II) macrocyclic complexes. The nitrosyl ruthenium(II)–ammines seem to depart from this correlation, forming another group.

A similar behavior is observed by plotting ν(NO) *versus* $E_{1/2}$(NO$^{+/\bullet}$). In both groups of complexes, a high ν(NO) frequency implies a high $E_{1/2}$(NO$^{+/\bullet}$) value, in agreement with the expected increase of the NO$^+$ character. This conclusion is more evident in the plot of ν(NO) *versus* ΣE_L, as shown in Fig. 6B. In this case, only a single linear correlation is observed, involving all the three series of complexes.

In situ, FTIR spectroelectrochemical measurements (Fig. 6B) revealed a shift of the νNO$^+$ vibrational peak at 1920 cm^{-1}, to 1890 cm^{-1}, in the direction of an increasing a NO^0 character for this ligand, in the reduced product. The relatively small shift of νNO ($\Delta\nu$ = 30 cm^{-1}) upon reduction, seems rather unusual, when compared with those observed for the [Ru(bipy)$_2$Cl(NO)]$^{2+/1+}$ ($\Delta\nu$ = 300 cm^{-1}) and [Ru(bipy)$_2$(AN)(NO)]$^{3+/2+}$ complexes ($\Delta\nu$ = 305 cm^{-1}).[32] Similar small shifts, however, have also been reported for the [Ru(dmgH)$_2$Cl(NO)]$^{0/-1}$ ($\Delta\nu$ = 23 cm^{-1}) [27] and [Ru(cyclam)Cl(NO)]$^{2+/1+}$ complexes ($\Delta\nu$ = 22 cm^{-1}).[3] In both cases, the low νNO values imply that in the oxidized form of the complex, the nitrosyl ligand has already a significant NO$^\bullet$ character; thus changing very little, after reduction. This is not our case. Instead, it should be noted that the reduction of the NO$^+$ ligand is accompanied by significant

Table 3 Selected EPR data for NO$^{\bullet}$ complexes

Compound	g_x	g_y	g_z	A_x/G	A_y/G	A_z/G
[a][RuCl(NO)(bpydip)]$^+$	1.991	2.027	1.889	32.3	16.9	14.8
[b][RuCl(NO)(cyclam)]$^+$	1.995	2.035	1.883	32.1	17.0	15.0
[c][RuCl(NO)(L)$_2$]$^+$	1.984	2.010	1.888	35.0	18.0	19.0
[d][Fe(CO)$_2$(NO)$_2$]$^-$	1.999	1.998	1.961	2.3	6.0	21.1
[e][Fe(CN)$_5$(NO)]$^{3-}$	2.008	1.997	1.930	26.0	30.0	8–10

[a] This work. [b] Ref. 3. [c] Ref. 20. [d] Ref. 39. [e] Ref. 40, L = $Et_2PC_4H_4PEt_2$.

changes in the vibrational spectrum of bpydip (Fig. 6B), reflecting the strong involvement of the NO and bpydip ligands in the electronic structure of the complex. In fact, from the delocalized nature of the HOMO and LUMO orbitals (Table 1), the formal reduction of the NO$^+$ ligand should be better described as the reduction of the whole complex. This would better explain the relatively small value of Δ*ν*(NO) for the *trans*-[RuCl(NO)(bpydip)]$^{2+}$ complex.

EPR spectra

A definite evidence for the formation of NO^0 species was obtained from the EPR spectra (Fig. 7) of the *trans*-[RuCl(NO$^{\bullet}$)(L)]$^{1+}$ complex, recorded after its reduction by Zn amalgam, in acetonitrile solution, under strictly anaerobic conditions, at 77 K. The results are summarized in Table 3, along with some selected literature data for NO$^{\bullet}$ complexes, for comparison purposes.[3,20,39,40] In agreement with the literature, the fine and nitrogen hyperfine structures are consistent with the formation of a reduced complex exhibiting predominantly NO$^{\bullet}$ character.[20] This conclusion is corroborated by preliminary photolysis experiments with the reduced complex, indicating the occurrence of photolabilization leading to the formation of NO and *trans*-[Ru(OH$_2$)$_2$(bpydip)]$^{2+}$ species as products.

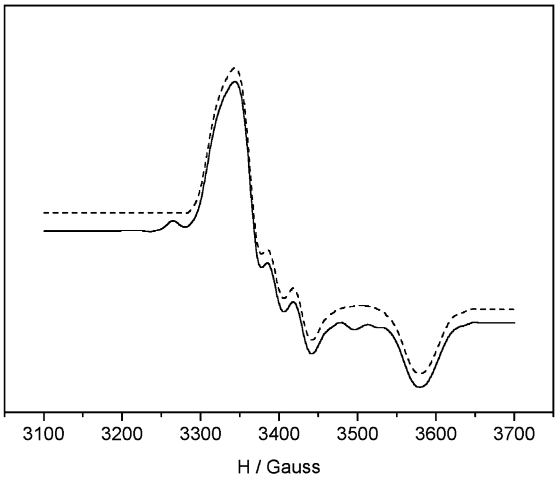

Fig. 7 Powder EPR spectrum of the reduced complex, *trans*-[RuCl(NO$^{\bullet}$)(bpydip)]$^+$, in acetonitrile solution at 77 K illustrating the NO$^{\bullet}$ character of the ligand. The dashed line is the simulated spectrum using the parameters shown in Table 3.[20]

Electrophilic behavior of *trans*-[RuCl(NO)(bpydip)](PF$_6$)$_2$

The [RuCl(NO)(bpydip)](PF$_6$)$_2$ complex shows relatively high *ν*(NO) stretching frequency (1920 cm^{-1}) indicating a high degree of positive charge residues on the coordinated nitrosyl group and consistent with the formulation of Ru^{II}–NO$^+$.[21] In fact, increasing nitrosyl stretching frequencies (ν_{NO} > 1850 cm^{-1}) generally correlate with the facility with which coordinated nitrosyl undergoes nucleophilic attack by OH$^-$, RO$^-$, RS$^-$, NH$_3$ and N$_2$H$_4$.[15]

In order to evaluate the electrophilic behavior of *trans*-[RuCl(NO)(bpydip)]$^{2+}$, the addition reaction of OH$^-$ ions, to yield *trans*-[RuCl(NO$_2$)(bpydip)], has been investigated in this work.

Conversion of *trans*-[RuCl(NO)(bpydip)]$^{2+}$ to *trans*-[RuCl(NO$_2$)-(bpydip)]

In the presence of water, the *trans*-[RuCl(NO)(bpydip)]$^{2+}$ complex convert rapid and quantitatively into the nitro species. In this case, the high reactivity of the nitrosyl group with water suggests a very high equilibrium constant for the convertion process in aqueous media. The rate of conversion of nitroso ⟶ nitro [(eqn. (1)] has been monitored spectrophotometrically in the temperature range 298–318 K in dry acetonitrile solvent and in the presence of a controlled concentration of water (50 times excess with respect to the complex).

$$[RuCl(NO)(bpydip)]^{2+} + H_2O \longrightarrow [RuCl(NO_2)(bpydip)] + 2H^+ \quad (1)$$

The spectral changes shown in Fig. 8 are consistent with a well behaved kinetic process, where the decay of the absorption bands of the nitrosyl complex in the UV/Visible region leads to the rise of a strong band at 530 nm associated with a MLCT transition in the [RuCl(NO$_2$)(bpydip)] product. A well defined isosbestic point is observed at 445 nm. The pseudo-first order rate constants (*k*) for this process, measured at several temperatures, were: k_{298} = 1.40 (± 0.02) × 10^{-2} s^{-1}; k_{308} = 2.60 (± 0.07) × 10^{-2} s^{-1} and k_{318} = 5.10 (± 0.06) × 10^{-2} s^{-1}. The calculated activation enthalpy and entropy were $\Delta H^{\neq}$ = 46.7 (± 1) kJ mol^{-1} and $\Delta S^{\neq}$ = 122 (± 4) J K^{-1} mol^{-1}.

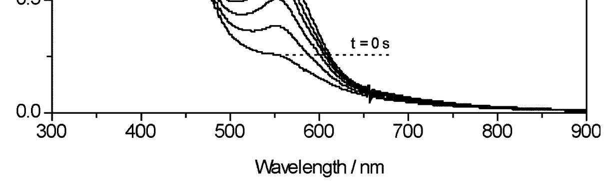

Fig. 8 Time evolution of the electronic spectra of a changing solution of [RuCl(NO)(bpydip)]$^{2+}$ ⟶ [RuCl(NO$_2$)(bpydip)] in dry acetonitrile and in the presence of a 50 times excess of water at 298 K.

Conclusion

The [RuCl(NO)(bpydip)]$^{2+/+}$ complex provides an interesting example of nitrosylcompound, where the NO$^{+/\bullet}$ character seems to be modulated by the tetradentate Schiff base. In its original form, the electron withdrawing properties of the bpydip ligand enhances the NO$^+$ character for the coordinated nitrosyl ligand, increasing its reactivity towards nucleophiles and even water. The monoelectronic reduction produces a characteristic $NO^{\bullet}$ species, exhibiting consistent vibrational and EPR spectra. The $NO^{\bullet}$ character, responsible for the typical EPR signals, seems to be modulated by the bpydip ligand, making the reduction potential for the $NO^{+} + e \longrightarrow NO^{\bullet}$ process very accessible, even to mild biological reducing agents.

Acknowledgements

We thank FAPESP and CNPq for financial support.

References

1 J. M. Slocik, M. S. Ward and R. E. Shepherd, *Inorg. Chim. Acta*, 2001, **317**, 290.
2 L. G. F. Lopes, A. Wieraszko, Y. El-Sherif and M. J. Clarke, *Inorg. Chim. Acta*, 2001, **312**, 15.
3 D. R. Lang, J. A. Davis, L. G. F. Lopes, A. A. Ferro, L. C. G. Vasconcellos, D. W. Franco, E. Tfouni, A. Wieraszko and M. J. Clarke, *Inorg. Chem.*, 2000, **39**, 2294.
4 C. W. B. Bezerra, S. C. Silva, M. T. P. Gambardella, R. H. A. Santos, L. M. A. Plicas, E. Tfouni and D. W. Franco, *Inorg. Chem.*, 1999, **38**, 5660.
5 J. W-S. Hui and W.-T. Wong, *Coord. Chem. Rev.*, 1998, **172**, 389.
6 S.-M. Lee and W.-T. Wong, *Coord. Chem. Rev.*, 1997, **164**, 415.
7 S. Moncada, R. M. J. Palmer and E. A. Higgs, *Pharmacol. Rev.*, 1991, **43**, 109.
8 G. B. Richter-Addo and P. Legzdins, in *Metal Nitrosyls*, Oxford University Press, New York, 1992.
9 W. R. Scheidt and M. K. Ellison, *Acc. Chem. Res.*, 1999, **32**, 350.
10 C. E. Cooper, *Biochim. Biophys. Acta*, 1999, **1411**, 290.
11 A. Wieraszko, M. J. Clarke, D. R. Lang, L. G. F. Lopes and D. W. Franco, *Life Sci.*, 2001, **68**, 1535.
12 D. A. Wink and J. B. Mitchell, *Free Radical Biol. Med.*, 1998, **25**, 434.
13 E. Culotta and D. E. Koshland, *Science*, 1992, **258**, 1862.
14 L. J. Ignarrow, *Pharm. Res.*, 1989, **6**, 651.
15 J. H. Enemark and R. D. Felthan, *Coord. Chem. Rev.*, 1974, **13**, 339.
16 I. A. Bagatin and H. E. Toma, *Transition Met. Chem.*, 1996, **21**, 71.
17 S. S. S. Borges, C. U. Davanzo, E. E. Castellano, J. Z-Schpector, S. C. Silva and D. W. Franco, *Inorg. Chem.*, 1998, **37**, 2670.
18 M. G. Gomes, C. U. Davanzo, S. C. Silva, L. G. F. Lopes, P. S. Santos and D. W. Franco, *J. Chem. Soc., Dalton Trans.*, 1998, 601.
19 Y. Chen, F.-T. Lin and R. E. Shepherd, *Inorg. Chem.*, 1999, **38**, 973.
20 B. R. McGarvey, A. A. Ferro, E. Tfouni, C. W. B. Bezerra, I. A. Bagatin and D. W. Franco, *Inorg. Chem.*, 2000, **39**, 3577.
21 B. Mondal, H. Paul, V. G. Puranik and G. K. Lahiri, *J. Chem. Soc., Dalton Trans.*, 2001, 481.
22 E. A. Seddon and K. R. Seddon, in *The Chemistry of Ruthenium*, Elsevier, New York, 1984.
23 A. Juris, V. Balzani, F. Barigelletti, S. Campagna, P. Belser and A. von Zelewsky, *Coord. Chem. Rev.*, 1988, **84**, 85.
24 T. G. Campbell and F. L. Urbach, *Inorg. Chem.*, 1973, **12**, 1836.
25 S. Choudhury, M. Kakoti, A. K. Deb and S. Goswami, *Polyhedron*, 1992, **11**, 3183.
26 B. Kratochvil, E. Lorah and C. Garber, *Anal. Chem.*, 1969, **41**, 1793.
27 I. A. Bagatin and H. E. Toma, *Spectrosc. Lett.*, 1996, **29**, 1409.
28 J. H. Espenson, in *Chemical Kinetics and Reaction Mechanisms*, McGraw-Hill, New York, 1995.
29 M. J. S. Dewar, E. G. Zoebisch, E. F. Healy and J. J. P. Stewart, *J. Am. Chem. Soc.*, 1985, **107**, 3902; M. J. S. Dewar and K. M. Dieter, *J. Am. Chem. Soc.*, 1986, **108**, 8075; J. J. P. Stewart, *J. Comp. Aided Mol. Design*, 1990, **4**, 1; J. E. Ridley and M. C. Zerner, *Theor. Chim. Acta*, 1973, **32**, 111; J. E. Ridley and M. C. Zerner, *Theor. Chim. Acta*, 1976, **42**, 223; A. D. Bacon and M. C. Zerner, *Theor. Chim. Acta*, 1979, **53**, 21; M. C. Zerner, G. H. Loew, R. F. Kirchner and U. T. Mueller-Westerhoff, *J. Am. Chem. Soc.*, 1980, **102**, 589.
30 M. Goto, Y. Ishikawa, T. Ishihara, C. Nakatake, T. Higuchi, H. Kurosaki and V. L. Goedken, *Chem. Commun.*, 1997, 539.
31 S. I. Gorelsky, S. C. Silva, A. B. P. Lever and D. W. Franco, *Inorg. Chim. Acta*, 2000, **300–302**, 698.
32 R. W. Callahan and T. J. Meyer, *Inorg. Chem.*, 1977, **16**, 574.
33 I. A. Bagatin and H. E. Toma, *Transition Met. Chem.*, 2000, **25**, 686.
34 W. A. Cramer and D. B. Knaff, in *Energy Transduction in Biological Membranes: A Textbook of Bioenergetics*, ed. Charles R. Cantor, Springer, New York, 1990.
35 E. S. Dodsworth, A. A. Vleck and A. B. P. Lever, *Inorg. Chem.*, 1994, **33**, 1045.
36 L. G. F. Lopes, M. G. Gomes, S. S. S. Borges and D. W. Franco, *Aust. J. Chem.*, 1998, **51**, 865.
37 A. B. P. Lever, *Inorg. Chem.*, 1990, **29**, 1271.
38 M. J. Clarke and J. B. Gaul, *Struct. Bonding*, 1993, **81**, 147.
39 C. Couture, J. R. Morton, K. F. Preston and S. J. Strach, *J. Magn. Reson.*, 1980, **41**, 88.
40 M. C. R. Symons, D. X. West and J. G. Wilkinson, *Inorg. Chem.*, 1976, **15**, 1022.